

# Geophysical Research Letters<sup>®</sup>

## RESEARCH LETTER

10.1029/2023GL108090

### Key Points:

- This study develops a diagnostic approach for untangling cloud-land relationships across distinct cloud coupling regimes
- Field observations are utilized to assess performances of reanalysis data in representing cloud-land interaction across different regimes
- Findings emphasize the importance of differentiating cloud coupling regimes in observational and modeling studies of boundary layer clouds

### Supporting Information:

Supporting Information may be found in the online version of this article.

### Correspondence to:

Z. Li and T. Su,  
zhanqing@umd.edu;  
su10@hnl.gov

### Citation:

Su, T., Li, Z., Zhang, Y., Zheng, Y., & Zhang, H. (2024). Observation and reanalysis derived relationships between cloud and land surface fluxes across cumulus and stratiform coupling over the Southern Great Plains. *Geophysical Research Letters*, 51, e2023GL108090. <https://doi.org/10.1029/2023GL108090>

Received 28 DEC 2023

Accepted 23 MAR 2024

### Author Contributions:

**Conceptualization:** Tianning Su,

Zhanqing Li, Youtong Zheng

**Data curation:** Tianning Su

**Funding acquisition:** Zhanqing Li,

Yunyan Zhang

**Investigation:** Tianning Su,

Haipeng Zhang

**Methodology:** Tianning Su,

Yunyan Zhang

**Project administration:** Zhanqing Li,

Yunyan Zhang

**Resources:** Tianning Su

**Supervision:** Zhanqing Li, Yunyan Zhang

**Validation:** Tianning Su




**Visualization:** Tianning Su

© 2024. The Authors.

This is an open access article under the terms of the [Creative Commons Attribution License](https://creativecommons.org/licenses/by/4.0/), which permits use,

distribution and reproduction in any medium, provided the original work is properly cited.

## Observation and Reanalysis Derived Relationships Between Cloud and Land Surface Fluxes Across Cumulus and Stratiform Coupling Over the Southern Great Plains

Tianning Su<sup>1,2</sup> , Zhanqing Li<sup>1</sup> , Yunyan Zhang<sup>2</sup>, Youtong Zheng<sup>3,4</sup> , and Haipeng Zhang<sup>1</sup> 

<sup>1</sup>AOSC & ESSIC, University of Maryland at College Park, College Park, MD, USA, <sup>2</sup>Lawrence Livermore National Laboratory, Livermore, CA, USA, <sup>3</sup>Department of Earth and Atmospheric Science, University of Houston, Houston, TX, USA, <sup>4</sup>Institute for Climate and Atmospheric Science, University of Houston, Houston, TX, USA

**Abstract** Understanding interactions between low clouds and land surface fluxes is critical to comprehending Earth's energy balance, yet their relationships remain elusive, with discrepancies between observations and modeling. Leveraging long-term field observations over the Southern Great Plains, this investigation revealed that cloud-land interactions are closely connected to cloud-land coupling regimes. Observational evidence supports a dual-mode interaction: coupled stratiform clouds predominate in low sensible heat scenarios, while coupled cumulus clouds dominate in high sensible heat scenarios. Reanalysis data sets, MERRA-2 and ERA-5, obscure this dichotomy owing to a shortfall in representing boundary layer clouds, especially in capturing the initiation of coupled cumulus in high sensible heat scenarios. ERA-5 demonstrates a relatively closer alignment with observational data, particularly in capturing relationships between cloud frequency and latent heat, markedly outperforming MERRA-2. Our study underscores the necessity of distinguishing different cloud coupling regimes, essential to the understanding of their interactions for advancing land-atmosphere interactions.

**Plain Language Summary** Low cloud interactions with the Earth's surface in the Southern Great Plains are examined to understand the coupling between low clouds and the land surface. Clouds play a major role in Earth's radiation energy balance and therefore the climate system, yet the cloud-land interaction relationship is complicated and not well-understood. Based on analyses of long-term field observations, we find that cloud-land interactions in this region are closely related to cloud-land coupling regimes. Observational evidence supports a dual-mode interaction: coupled stratiform clouds that dominate in low sensible heat states and coupled cumulus that dominate in high sensible heat states. The reanalysis data sets exhibit a common shortcoming of a deficit in boundary layer cloud parameterization, with a poorer representation of the initiation of coupled cumulus especially. This study highlights the importance of understanding the different cloud coupling regimes that interact with the land, which is essential for advancing weather and climate models.

## 1. Introduction

Low clouds are key players in Earth's climate, influencing radiative balance and climate feedback loops. Continental low-level clouds are influenced by the land surface via processes occurring within the planetary boundary layer (PBL) (Berg & Kassianov, 2008; Betts, 2009; Fast, Berg, Feng, et al., 2019; Golaz et al., 2002; Guo et al., 2019; Schumacher & Funk, 2023; Teixeira & Hogan, 2002; Yang et al., 2019; Zhang et al., 2017). These clouds often emerge within the PBL's entrainment zone under convective conditions, yet their coupling with the land surface is complex and presents challenges in accurate determination and understanding (T. Su et al., 2022). Thus, a comprehensive examination of how terrestrial processes affect cloud evolution is warranted to understand the coupling of low-level clouds with the land surface (Bretherton et al., 2007; Moeng et al., 1996; T. Su & Li, 2024; T. Su et al., 2023; Xian et al., 2023; Zheng et al., 2021).

Extensive research has been carried out to investigate cloud-land interactions, highlighting the important roles of land surface heterogeneity, evaporative fraction, and soil moisture (Qian et al., 2023; Tang et al., 2019; Yue et al., 2017). Specifically, multiple studies have documented how land surface heterogeneity impacts the formation of shallow convection and development (Lee et al., 2019; Rieck et al., 2014; Xiao et al., 2018). Fast, Berg, Alexander, et al. (2019) and Tao et al. (2019) have elucidated the strength of land-atmosphere interactions and their important roles in modulating convective cloud formation and evolution. As the majority of these studies

**Writing – original draft:** Tianning Su  
**Writing – review & editing:** Tianning Su,  
Zhanqing Li, Yunyan Zhang,  
Youtong Zheng, Haipeng Zhang

have focused on local convection or cumulus, the wide range of cloud types and their interactions with the land surface present a complex and multifaceted challenge (Poll et al., 2022; Sakaguchi et al., 2022; Tao et al., 2021). It is essential to delve into these characteristics and dissect the cloud-land relationships across different regimes to achieve a more detailed understanding of these interactions.

Cloud variables in reanalysis data have also been extensively utilized in numerous studies (Cesana et al., 2015; H. Su et al., 2013), and have undergone detailed evaluations for the vertical structure and spatial variations (Dolinar et al., 2016; Free et al., 2016; Liu & Key, 2016). Several studies have reported the underestimation of low-level cloud fraction in popular reanalysis data sets, such as the European Centre for Medium-Range Weather Forecasts' fifth-generation global reanalysis (ERA-5), across different regions (Danso et al., 2019; Miao et al., 2019; Peng et al., 2019). Besides, reanalysis data sets face significant challenges in accurately representing the complex interactions between low clouds and the land surface (Betts et al., 2006; Tao et al., 2021; Wang et al., 2023). A gap exists in specifically assessing how these data sets capture cloud-land-surface coupling, particularly under stratiform regimes. Consequently, further investigation is warranted into the effectiveness of reanalysis products in representing the relationships between clouds and land surface fluxes across different coupling regimes.

Our study addresses two primary objectives: firstly, to develop a diagnostic approach for untangling cloud-land relationships across distinct cloud coupling regimes; and secondly, to evaluate the performance of prevailing reanalysis data sets in representing these relationships across different cloud regimes. Utilizing field observations over the Atmospheric Radiation Measurement (ARM) Southern Great Plains (SGP) site, we investigate the interactions between low clouds and land surface fluxes and highlight the discrepancies with reanalysis data sets for different cloud regimes, including coupled stratiform, coupled cumulus, and decoupled clouds.

## 2. Data and Method

### 2.1. Observational and Reanalysis Data Set

The ARM program, funded by the U.S. Department of Energy, has been operational at the SGP site in Oklahoma (36.607°N, 97.488°W) for decades. We use long-term data (1998–2020) over the SGP, including the Active Remote Sensing of Clouds (ARSCL, Clothiaux et al., 2000, 2001; Kollias et al., 2020), thermodynamic profiles from radiosonde, in-situ surface flux measurements, and meteorological data recorded at the surface (Cook, 2018; Xie et al., 2010). We further use reanalysis data sets from the ERA-5 (Hersbach et al., 2020) and Modern-Era Retrospective analysis for Research and Applications Version 2 (MERRA-2, Gelaro et al., 2017). As the state-of-art reanalysis data, the ERA-5 is produced by the Integrated Forecasting System and a data assimilation system at a fine spatial resolution of  $0.25^\circ \times 0.25^\circ$ . Meanwhile, the MERRA-2 offers atmospheric and land information at a resolution of  $0.5^\circ \times 0.625^\circ$  (Randles et al., 2017). An important difference between the ERA-5 and MERRA-2 is the cloud parameterization: ERA-5 uses a prognostic cloud scheme (Tiedtke, 1993) that accounts for the impacts from previous time steps whereas MERRA-2 uses a diagnostic cloud scheme. The procurement, processing, and quality assurance steps for observational and reanalysis data sets are further detailed in Text S1 in Supporting Information S1.

### 2.2. Identification of Cloud Coupling Regimes

T. Su et al. (2022) developed a micropulse lidar-based approach to discern the cloud-land coupling by accounting for the vertical coherence and temporal continuity of PBL height (Planetary Boundary Layer Height (PBLH)). Clouds are defined as coupled when the turbulence originating from the surface is able to reach the cloud base, thereby influencing its evolution, resulting in a turbulence-facilitated linkage among surface fluxes, PBL, and the cloud. We differentiate between coupled and decoupled low-level clouds using PBLH, cloud base, and lifting condensation level (LCL). The method for calculating PBLH is detailed in T. Su et al. (2020) which has been used to develop a PBLH climatological data set at the central facilities of SGP. LCL values are calculated using the method outlined in Romps (2017). Coupled clouds are identified by the alignment of cloud base height with the lidar-detected PBL top and LCL within a defined range, while decoupled clouds, which form independently of surface-driven updrafts, are indicated by a lack of this alignment.

Following the determination of cloud-land coupling, we exclude precipitation events exceeding  $0.1 \text{ mm hr}^{-1}$  to prevent distortion in lidar signals and surface flux measurements. The study focuses on data from 09:00 to 15:00 Local Time (LT) to avoid the late afternoon period when the PBL typically begins to decay. We exclude the

coexistence of coupled and decoupled low clouds during this period and further implement a classification into cumulus and stratiform categories among coupled cloud days. For coupled cumulus, two conditions are implemented in line with practices from previous studies (Lareau et al., 2018; Zhang & Klein, 2010, 2013): (a) cloud formations must emerge after sunrise without low clouds at 08:00 LT to make sure that clouds are driven by local convection; (b) there is absence of overcast clouds. Coupled stratiform clouds are characterized by prolonged overcast clouds, which last more than 3 hr. Overcast low-level clouds have a cloud fraction of more than 90% based on ASRSL data.

Figure S1 in Supporting Information S1 showcases these cloud regimes, with coupled cumulus manifesting as discrete cellular formations in satellite imagery, and coupled stratiform clouds displaying broad, extensive coverage starting from the previous night. Meanwhile, decoupled clouds are distinguished by their separation from surface-driven PBL activity. Applying this methodological framework has led to the identification of 631 days marked by coupled cumulus and 470 days with coupled stratiform clouds across all seasons. In addition, we have distinguished 578 days with decoupled clouds across two decades, excluding instances with mixed coupled and decoupled low clouds. Compared to the conventional approaches focused on identifying the specific types of clouds (e.g., cumulus or stratocumulus), our approach delineates different cloud-land coupling regimes, encompassing both coupled/decoupled states and cumulus/stratiform regimes. This enables a comprehensive analysis of cloud-land interactions, examining these relationships through the perspective of cloud-land coupling.

### 3. Results

#### 3.1. Overall Relationship Between Cloud Occurrence Frequency and Surface Fluxes

Our investigation begins by exploring the connection between the frequency of low cloud occurrences and surface sensible and latent heat fluxes. The evaluation criterion for low cloud occurrence is based on hourly cloud fraction where the maximum value between the surface and 700 hPa exceeds a 1% threshold. This study analyzes hourly mean data, with hourly low cloud occurrence categorized as 0 or 1. The cloud frequency is further calculated by dividing the sum by the total number of hours analyzed. This analysis incorporates data from both observational sources and the reanalysis data sets of ERA-5 and MERRA-2, as detailed in Figure 1. For the overall relationship, the same precipitation filter of  $0.1 \text{ mm hr}^{-1}$  has been applied to the observation, ERA-5, and MERRA-2. Observational findings depicted in Figures 1a and 1b showcase a dual-mode interaction: cloud frequencies initially diminish at lower sensible heat levels and subsequently augment with an increase in sensible heat.

When extending the analysis to reanalysis data sets, different responses of cloud to surface fluxes emerge (Figures 1c–1f). The correlation between surface fluxes observed and those within reanalysis data sets is presented in Figure S2 in Supporting Information S1. While ERA-5 partially captures the essence of the observed cloud-land relationships, particularly for latent heat, it still exhibits discrepancies in cloud frequency concerning sensible heat. ERA-5 data reflects a trend of decreasing cloud frequency with rising sensible heat, compared to the dual-mode interaction in the observations.

MERRA-2's response, however, is notably different; it presents a systematic underestimation of cloud occurrences across all surface flux ranges. Figure S3 in Supporting Information S1 accentuates this point by showing that both reanalysis data sets, especially MERRA-2, consistently underrepresent the average low cloud fractions across the spectrum of sensible and latent heat fluxes compared to observational data.

#### 3.2. Characteristics for Different Cloud Regimes

To elucidate the complex relationship between cloud presence and terrestrial influences, Figure 2 presents the changes of cloud occurrence frequency (COF) relative to surface sensible heat for different cloud regimes. By excluding days where low cloud regimes intermingle, we isolate the distinct behavioral signatures of each regime among days with coupled/decoupled scenarios and clear-sky. In the juxtaposition of reanalysis data sets against field observations, we examine the variation in cloud frequency under different levels of sensible heat in Figure 2. For comparison, these regimes of days are classified solely based on observational data and the relationships are calculated from observation and reanalysis data for the same samples.

Coupled stratiform clouds are characterized by their extensive coverage and cloud shading effects, predominating under low sensible heat conditions. As a result, there is a notable decrease in sensible heat concurrent with the increase in cloud frequency, as illustrated in Figures 2a–2c. These clouds are associated with a well-mixed and

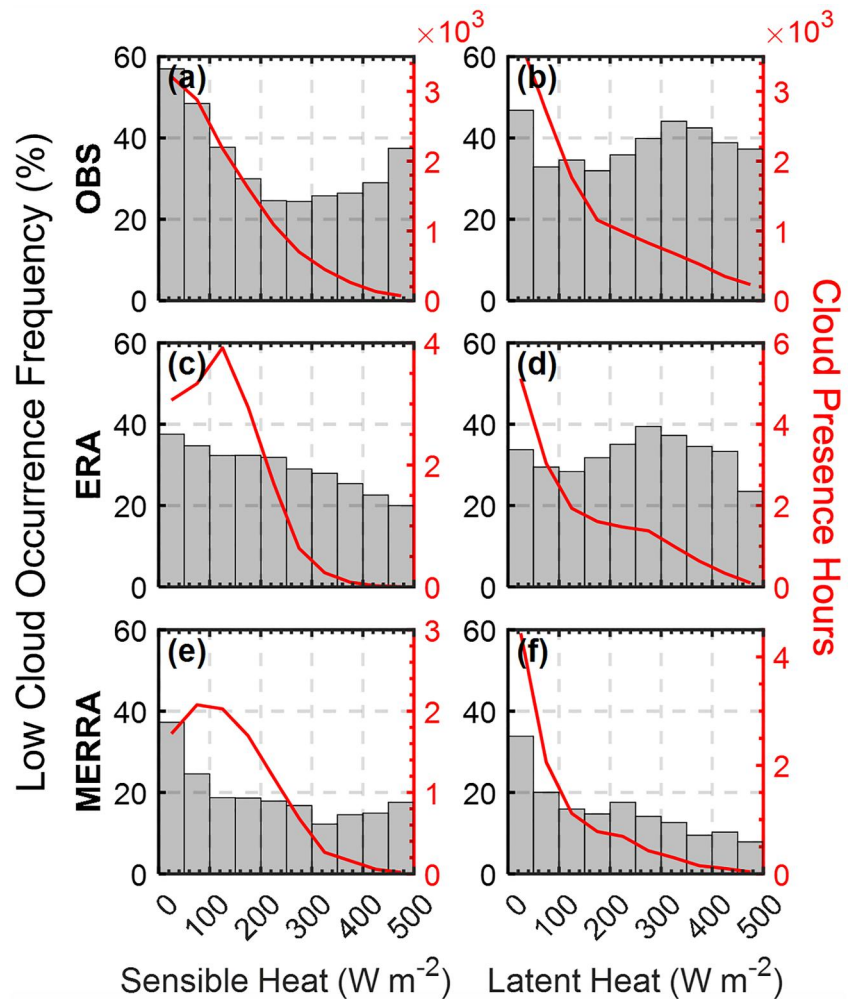


**Figure 1.** Comparison of observations and reanalysis for the relationships between low clouds and surface fluxes. Histograms represent the average frequency of low cloud occurrences binned by (a, c, e) surface sensible heat and (b, d, f) latent heat flux during 09:00–15:00 Local Time. Red lines indicate the number of hours with low cloud occurrence within each flux bin. Cases with precipitation exceeding  $0.1 \text{ mm hr}^{-1}$  are excluded from analyses. The (a and b) first, (c and d) second, and (e and f) third rows correspond to observations, ERA-5, and MERRA-2 respectively.

unstable sub-cloud layer, indicative of a dynamic exchange of heat and moisture with the underlying surface, as depicted in Figure S4 in Supporting Information S1. The presence of widespread overcasting, often concurrent with lower sensible heat, reinforces the persistence of stratiform clouds by mitigating the drying effects of entrainment.

In the realm of coupled cumulus, an increase in sensible heat is linked to enhanced cloud formation, as surface heating intensifies convective activity within the PBL. During days when these clouds are present, ERA-5 data tend to underestimate the frequency of locally generated convection under high sensible heat scenarios, as reflected in Figures 2d and 2e. MERRA-2 demonstrates a significant deviation from observed patterns, consistently missing a large fraction of low clouds (Figure 2f). Decoupled clouds exhibit a more complex relationship with surface sensible heat (Figures 2g–2i). Although they do not interact directly with PBL thermodynamics, they exert a cloud shading effect, leading to a suppression of surface sensible heat.

Figure 3 shows the relationships between cloud and latent heat. In analogy with the trends observed for sensible heat, coupled stratiform clouds demonstrate a diminishing frequency with increasing latent heat. On the other hand, coupled cumulus clouds tend to occur more frequently as latent heat increases, indicative of a conducive environment for cloud coupling, possibly through mechanisms such as lowering the LCL alongside PBL growth.



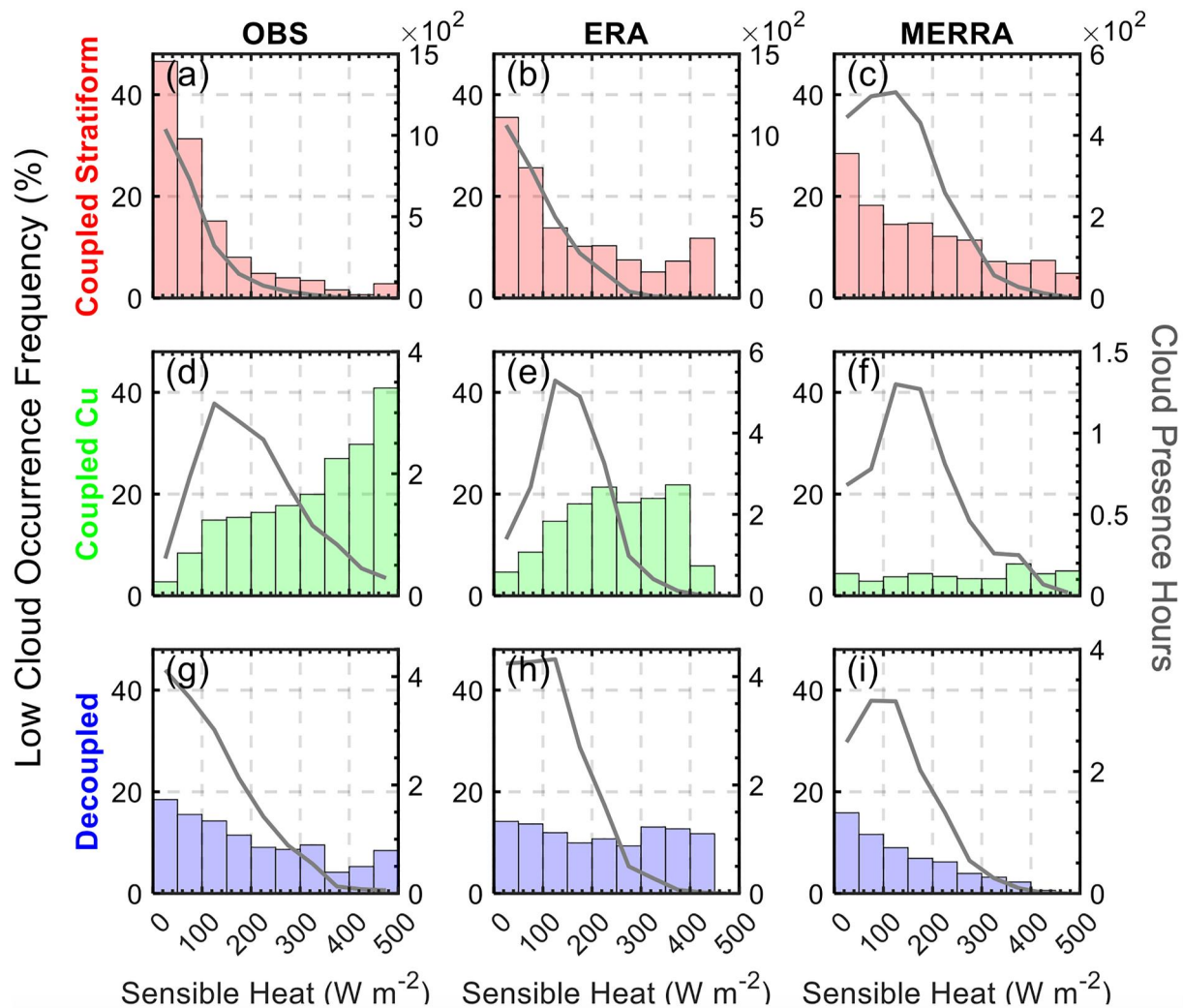


**Figure 2.** Cloud occurrence frequency and surface sensible heat relationships segregated by conditions of cloud regimes during 09:00–15:00 Local Time. The histograms display the average frequency of different cloud types binned by surface sensible heat flux for observational (OBS), ERA reanalysis, and MERRA reanalysis data sets. Panels (a–c) showcase coupled stratiform clouds, panels (d) to (f) depict coupled cumulus clouds, and panels (g–i) present decoupled clouds. Gray lines indicate the number of hours with low cloud occurrence within each flux bin.

This highlights that moderate to strong latent heat particularly promotes cloud formation coupling. To address the gap between grid and point data, we employed surface fluxes gridded to a spatial resolution of  $0.25^\circ \times 0.25^\circ$  for analyzing the cloud-land relationships, revealing that the patterns of these relationships exhibit similarity across both the gridded and point flux measurements (Figures S5 and S6 in Supporting Information S1). In addition, stratiform cloud frequency generally increases with the evaporative fraction, emphasizing latent heat's role in their formation, while both ERA-5 and MERRA-2 inaccurately depict a decline in cloud frequency across evaporative fraction ranges and also fail to accurately represent cumulus formation at lower evaporative fraction values, which are primarily driven by sensible heat (Figure S7 in Supporting Information S1).

The diurnal variation in cloud fraction across the different regimes is further illustrated in Figure 4, which underscores the notable biases present in reanalysis data sets. MERRA-2 notably underestimates low-level cloud fractions. Despite a similar pattern, ERA-5 struggles to represent local cumulus convection and decoupled cloud scenarios with insufficient cloud fraction. Such underrepresentation of boundary layer clouds culminates in a generalized underestimation of low clouds within both MERRA-2 and ERA-5 (Figure S8 in Supporting Information S1). The underestimation in the low cloud fraction can also lead to a weak surface cooling effect in reanalysis data.

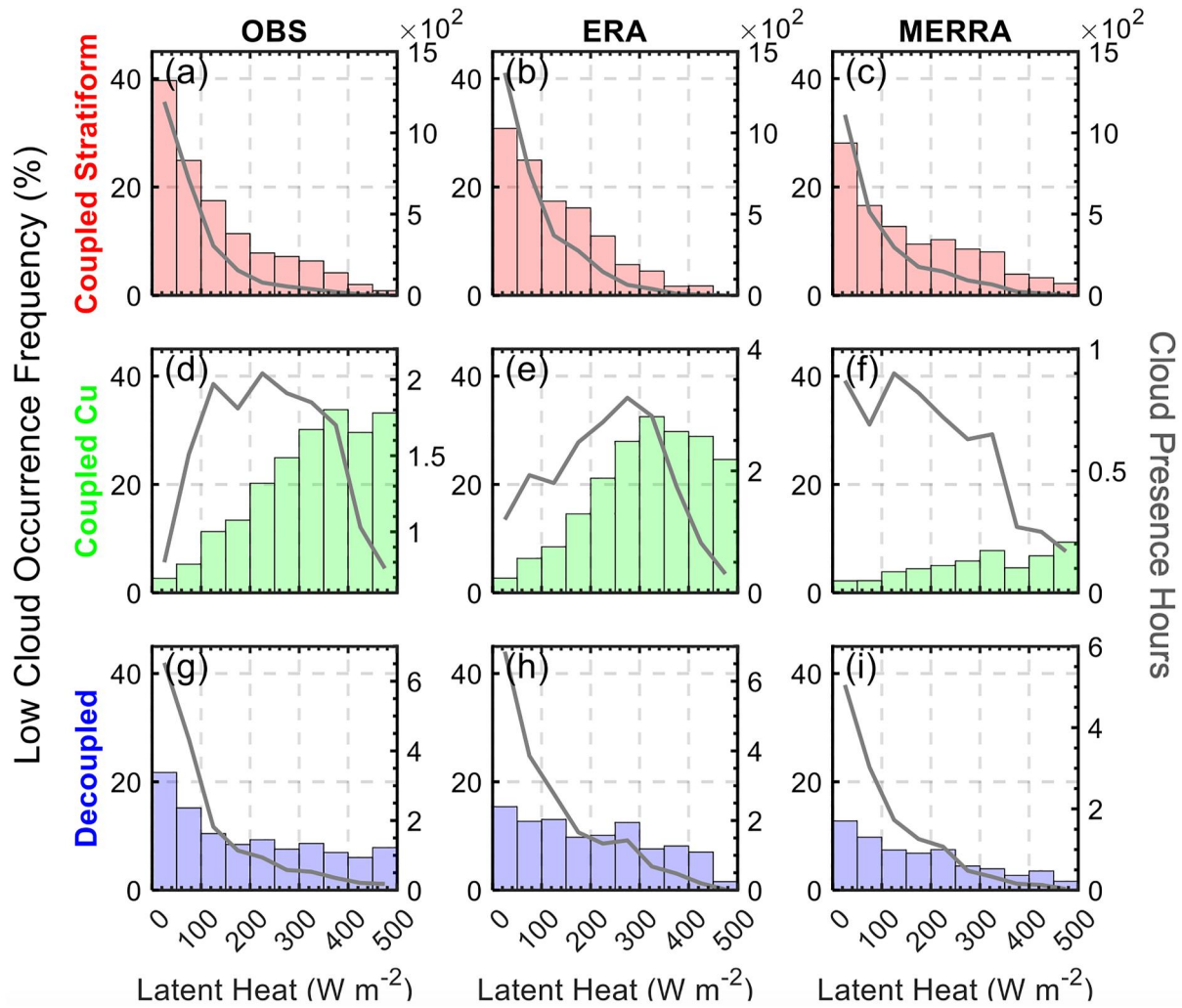


**Figure 3.** Similar to Figure 2, but depicting the relationships between low cloud occurrence frequency and surface latent heat fluxes.

Our results are related to prior studies that highlight diurnal biases in convection over the central United States, particularly the challenges in accurately capturing local convection and the insufficient triggering of cumulus, as detailed in studies by Tao et al. (2021, 2023). Their studies also noted the shortfall in triggering shallow cumulus clouds, contributing to the biases in convection patterns.

### 3.3. Meteorological Triggers for Cloud Formation Across Regimes

Cloud development across various coupling regimes is linked to essential meteorological factors, particularly atmospheric instability and humidity, as indicated by PBLH and surface relative humidity ( $RH_{sfc}$ ). Figure 5a presents the coupling-decoupling difference, calculated as the difference between the frequencies of coupled and decoupled clouds, and examines its correlations with changes in PBLH and  $RH_{sfc}$ . Their relationships are also influenced by sensible heat marked in the gray-scale dots showing the connections between PBLH and  $RH_{sfc}$  under an array of sensible heat conditions. Figure 5b indicates the corresponding variations in the frequency of low clouds under different values of PBLH and  $RH_{sfc}$ .

Distinct domains emerge within the coupled cloud zone: more coupled stratiform clouds are prevalent in environments under higher  $RH_{sfc}$  and lower PBLH, typically associated with lower sensible heat conditions. Conversely, coupled cumulus clouds flourish under opposite conditions (i.e., lower  $RH_{sfc}$  and higher PBLH) suggestive of higher sensible heat and strong convection. Decoupled clouds, inferred from their negative coupling-decoupling differences, tend to occur toward lower PBLH across a broader RH spectrum, indicating

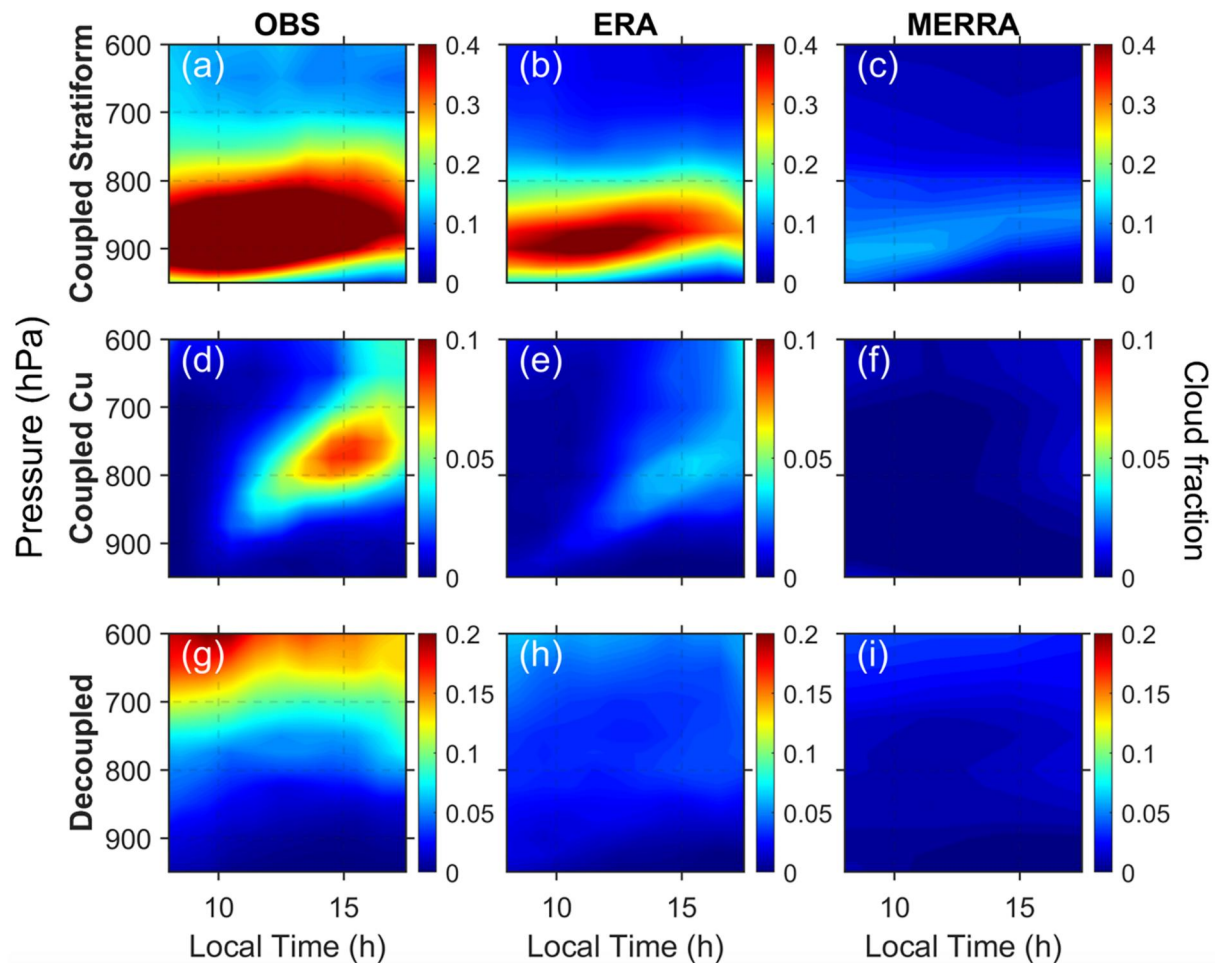


**Figure 4.** Diurnal variation of cloud fraction with atmospheric pressure across different cloud regimes in observations and reanalysis data. This figure presents contour plots that display the variation of cloud fraction during the daytime at various atmospheric pressures for three distinct scenarios: coupled stratiform clouds, coupled cumulus, and decoupled clouds. Each row represents one of the cloud scenarios, with observational data (OBS) in the first column, ERA reanalysis data in the second column, and MERRA reanalysis data in the third column.

their formation is less contingent on surface-induced convective processes. From low to high sensible heat, cloud regimes transit from coupled stratiform to coupled cumulus clouds.

Figures 5c and 5d present comparative analyses of the frequency of clouds vis-à-vis PBLH and  $RH_{sf,c}$ , extracted from reanalysis data sets. Notably, both the occurrence and fraction of clouds are misrepresented in MERRA-2. While the ERA-5 clouds generally bear closer resemblance to the observed clouds, but still differ considerably in the occurrences of both coupled stratiform clouds and coupled cumulus. The underrepresentation of cumulus by the reanalysis stems from inadequate PBL development under high sensible heat scenarios (Figures 5c and 5d). Meanwhile, the RH is notably lower for the low sensible heat scenarios, which are linked with stratiform clouds. The systematic underestimation in RH can contribute to the overall underestimation of both cumulus and stratiform clouds, as illustrated in Figure S9 in Supporting Information S1, further hindering the triggering of coupled clouds. These findings underscore the critical need for enhancing the accuracy of surface flux and humidity representation in reanalysis data sets, alongside refining the parametrization of their effects on convection.

#### 4. Discussion and Conclusions

In this study, we dissect the complex relationships between low clouds and surface fluxes over the SGP. Building on previous studies that were primarily focused on cloud-land interactions within shallow cumulus, we demonstrate that both the cumulus and stratiform regimes represent distinct yet interconnected modes of cloud-

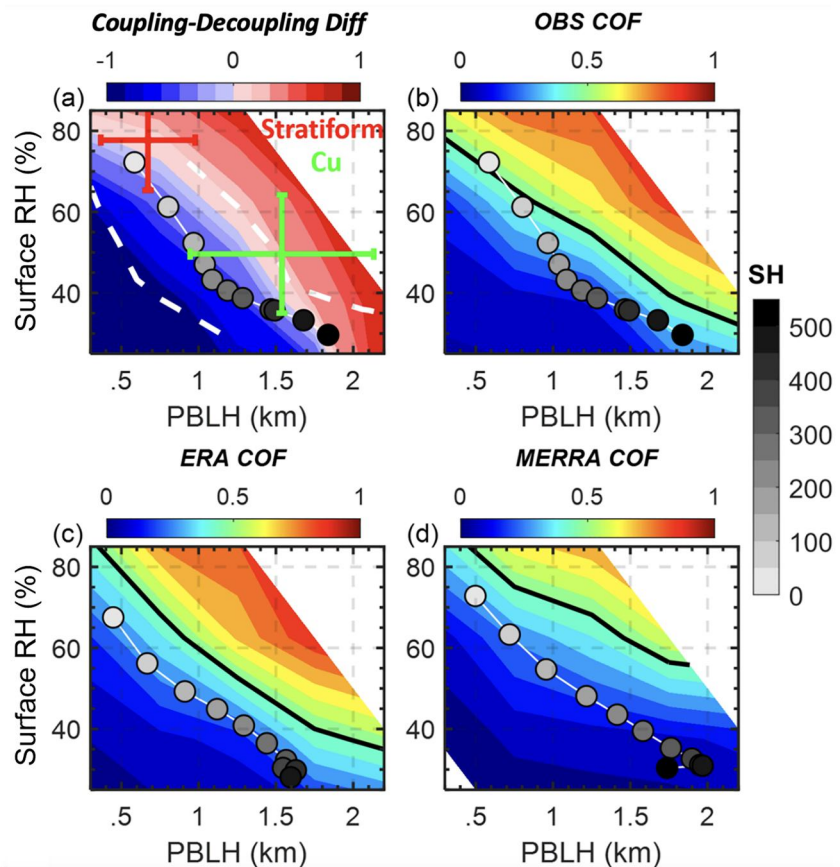


**Figure 5.** (a) The differences between the frequencies of coupled and decoupled clouds (former minus latter) under the different ranges of Planetary Boundary Layer Height (PBLH) and surface relative humidity ( $RH_{sfc}$ ) (b)–(d) The values of the low cloud occurrence frequency (COF) correspond to PBLH and  $RH_{sfc}$  from (b) observations, (c) ERA-5, and (d) MERRA-2. In (a), the means and standard deviations of stratiform clouds and cumulus are marked. The gray-scale dots indicate the averages of PBLH and  $RH_{sfc}$  for different sensible heat values. The dash white lines in (a) indicate the range of standard deviations of different PBLH for different sensible heat bins. The black line denoting the position of 50% COF.

land coupling. Consequently, we explore a bifurcated interaction pattern within the framework of cloud-land coupling, identifying that stratiform coupling prevails in low sensible heat conditions, while cumulus coupling becomes the leading regime in high sensible heat scenarios. Together, these findings portray the full paradigm of the coupling between cloud and land surface, occurring under various conditions. It follows from analyses of observations that meteorological conditions such as PBLH and  $RH_{sfc}$  are instrumental in cloud formation across different regimes, with transitions from stratiform to cumulus regimes leading to the overall pattern of cloud-land relationships.

Reanalysis data sets do not sufficiently capture the observed bifurcated interaction pattern and present a damped decline pattern in the cloud-land relationship. MERRA-2 consistently underestimates cloud frequency across various cloud regimes, with a particular shortfall in capturing the occurrence of coupled cumulus. ERA-5 generally exhibits a superior correlation with observational data, notably in the context of latent heat interactions. However, ERA-5 still shows discrepancies, especially with the frequency and initiation of coupled cumulus. Meanwhile, both reanalysis data sets fail to represent decoupled clouds accurately, as these clouds' formation mechanisms appear disconnected from local PBL processes.

This assessment of different cloud regimes underscores the significance of cloud coupling in analyzing cloud-land interactions. The initiation of convection in coupled cumulus is closely tied to surface processes on a sub-grid scale (Tian et al., 2022). As these cloud regimes respond to climate change, misrepresentation of these cloud dynamics within climate models could lead to uncertainties in predictions of climate sensitivity, as posited by Schneider et al. (2019). The emergence of global storm-resolving models with kilometer-scale resolutions, as



detailed in Satoh et al. (2005), Caldwell et al. (2021), and Hohenegger et al. (2023), may offer great potential for addressing these complex modeling challenges in cloud-land interactions.

### Data Availability Statement

Atmospheric Radiation Measurement radiosonde data, surface fluxes, and cloud masks are available online (ARM User Facility, 1994). The identification for different cloud regimes for the study period is publicly available (T. Su, 2023). The data of PBL are archived as an ARM product (T. Su & Li, 2023). Climate Data Store offers the ERA-5 reanalysis data (Hersbach et al., 2023). MERRA-2 reanalysis data can be downloaded online (GMAO, 2015).

### Acknowledgments

This work is supported by Grants from the U.S. DOE (DE-SC0022919), the National Science Foundation (AGS2126098), and NASA (80NSSC21K1980). Y. Zheng is supported by the DOE Early Career Grant (DE-SC0024185). Y. Zhang is supported by the DOE Atmospheric System Research Science Focus Area THREAD project. Work at LLNL is performed under the auspices of the U.S. DOE by Lawrence Livermore National Laboratory under Contract DE-AC52-07NA27344.

### References

- Atmospheric Radiation Measurement (ARM) User Facility. (1994). ARM best estimate data products (ARMBEATM). Southern Great Plains (SGP) central facility, Lamont, OK (C1). Compiled by C. Xiao and X. Shaocheng [Dataset]. *ARM Data Center*. <https://doi.org/10.5439/1333748>
- Berg, L. K., & Kassianov, E. I. (2008). Temporal variability of fair-weather cumulus statistics at the ACRF SGP site. *Journal of Climate*, 21(13), 3344–3358. <https://doi.org/10.1175/2007jcli2266.1>
- Betts, A. K. (2009). Land-surface-atmosphere coupling in observations and models. *Journal of Advances in Modeling Earth Systems*, 1(3), 4. <https://doi.org/10.3894/james.2009.1.4>
- Betts, A. K., Ball, J. H., Barr, A. G., Black, T. A., McCaughey, J. H., & Viterbo, P. (2006). Assessing land-surface-atmosphere coupling in the ERA-40 reanalysis with boreal forest data. *Agricultural and Forest Meteorology*, 140(1–4), 365–382. <https://doi.org/10.1016/j.agrformet.2006.08.009>
- Bretherton, C. S., Blossey, P. N., & Uchida, J. (2007). Cloud droplet sedimentation, entrainment efficiency, and subtropical stratocumulus albedo. *Geophysical Research Letters*, 34(3), L03813. <https://doi.org/10.1029/2006gl027648>
- Caldwell, P. M., Terai, C. R., Hillman, B., Keen, N. D., Bogenschütz, P., Lin, W., et al. (2021). Convection-permitting simulations with the E3SM global atmosphere model. *Journal of Advances in Modeling Earth Systems*, 13(11), e2021MS002544. <https://doi.org/10.1029/2021ms002544>
- Cesana, G., Waliser, D. E., Jiang, X., & Li, J. L. (2015). Multimodel evaluation of cloud phase transition using satellite and reanalysis data. *Journal of Geophysical Research: Atmospheres*, 120(15), 7871–7892. <https://doi.org/10.1002/2014jd022932>
- Clothiaux, E. E., Ackerman, T. P., Mace, G. G., Moran, K. P., Marchand, R. T., Miller, M. A., & Martner, B. E. (2000). Objective determination of cloud heights and radar reflectivities using a combination of active remote sensors at the ARM CART sites. *Journal of Applied Meteorology and Climatology*, 39(5), 645–665. [https://doi.org/10.1175/1520-0450\(2000\)039<0645:odocha>2.0.co;2](https://doi.org/10.1175/1520-0450(2000)039<0645:odocha>2.0.co;2)
- Clothiaux, E. E., Miller, M. A., Perez, R. C., Turner, D. D., Moran, K. P., Martner, B. E., et al. (2001). *The ARM millimeter wave cloud radars (MMCRs) and the active remote sensing of clouds (ARSCCL) value added product (VAP)* (No. DOE/SC-ARM/VAP-002.1). DOE Office of Science Atmospheric Radiation Measurement (ARM) Program (United States).
- Cook, D. R. (2018). *Energy balance Bowen ratio station (EBBR) instrument handbook* (No. DOE/SC-ARM/TR-037). DOE Office of Science Atmospheric Radiation Measurement (ARM) Program (United States).
- Danso, D. K., Anquetin, S., Diedhiou, A., Lavaysse, C., Koba, A., & Touré, N. D. E. (2019). Spatio-temporal variability of cloud cover types in West Africa with satellite-based and reanalysis data. *Quarterly Journal of the Royal Meteorological Society*, 145(725), 3715–3731. <https://doi.org/10.1002/qj.3651>
- Dolinar, E. K., Dong, X., & Xi, B. (2016). Evaluation and intercomparison of clouds, precipitation, and radiation budgets in recent reanalyses using satellite-surface observations. *Climate Dynamics*, 46(7–8), 2123–2144. <https://doi.org/10.1007/s00382-015-2693-z>
- Fast, J. D., Berg, L. K., Alexander, L., Bell, D., D'Ambro, E., Hubbe, J., et al. (2019). Overview of the HI-SCALE field campaign: A new perspective on shallow convective clouds. *Bulletin of the American Meteorological Society*, 100(5), 821–840. <https://doi.org/10.1175/bams-d-18-0030.1>
- Fast, J. D., Berg, L. K., Feng, Z., Mei, F., Newsom, R., Sakaguchi, K., & Xiao, H. (2019). The impact of variable land-atmosphere coupling on convective cloud populations observed during the 2016 HI-SCALE field campaign. *Journal of Advances in Modeling Earth Systems*, 11(8), 2629–2654. <https://doi.org/10.1029/2019ms001727>
- Free, M., Sun, B., & Yoo, H. L. (2016). Comparison between total cloud cover in four reanalysis products and cloud measured by visual observations at US weather stations. *Journal of Climate*, 29(6), 2015–2021. <https://doi.org/10.1175/jcli-d-15-0637.1>
- Gelaro, R., McCarty, W., Suárez, M. J., Todling, R., Molod, A., Takacs, L., et al. (2017). The Modern-Era Retrospective Analysis for Research and Applications, version 2 (MERRA-2). *Journal of Climate*, 30(14), 5419–5454. <https://doi.org/10.1175/jcli-d-16-0758.1>
- Global Modeling and Assimilation Office (GMAO). (2015). MERRA-2 tavg1\_2d\_rad\_Nx: 2d, 1-Hourly, Time-Averaged, Single-Level, Assimilation, Radiation diagnostics V5.12.4 [Dataset]. *Goddard Earth Sciences Data and Information Services Center (GES DISC)*. <https://doi.org/10.5067/Q9QM5PBNV1T>
- Golaz, J. C., Larson, V. E., & Cotton, W. R. (2002). A PDF-based model for boundary layer clouds. Part I: Method and model description. *Journal of the Atmospheric Sciences*, 59(24), 3540–3551. [https://doi.org/10.1175/1520-0469\(2002\)059<3540:apbmbf>2.0.co;2](https://doi.org/10.1175/1520-0469(2002)059<3540:apbmbf>2.0.co;2)
- Guo, J., Su, T., Chen, D., Wang, J., Li, Z., Lv, Y., et al. (2019). Declining summertime local-scale precipitation frequency over China and the United States, 1981–2012: The disparate roles of aerosols. *Geophysical Research Letters*, 46(22), 13281–13289. <https://doi.org/10.1029/2019gl085442>
- Hersbach, H., Bell, B., Berrisford, P., Biavati, G., Horányi, A., Muñoz Sabater, J., et al. (2023). ERA5 hourly data on pressure levels from 1940 to present [Dataset]. *Copernicus Climate Change Service (C3S) Climate Data Store (CDS)*. <https://doi.org/10.24381/cds.bd0915c6>
- Hersbach, H., Bell, B., Berrisford, P., Hirahara, S., Horányi, A., Muñoz-Sabater, J., et al. (2020). The ERA5 global reanalysis. *Quarterly Journal of the Royal Meteorological Society*, 146(730), 1999–2049. <https://doi.org/10.1002/qj.3803>
- Hohenegger, C., Korn, P., Linardakis, L., Redler, R., Schnur, R., Adamidis, P., et al. (2023). ICON-sapphire: Simulating the components of the Earth system and their interactions at kilometer and subkilometer scales. *Geoscientific Model Development*, 16(2), 779–811. <https://doi.org/10.5194/gmd-16-779-2023>

- Kollias, P., Bharadwaj, N., Clothiaux, E. E., Lamer, K., Oue, M., Hardin, J., et al. (2020). The ARM radar network: At the leading edge of cloud and precipitation observations. *Bulletin of the American Meteorological Society*, 101(5), E588–E607. <https://doi.org/10.1175/bams-d-18-0288.1>
- Lareau, N. P., Zhang, Y., & Klein, S. A. (2018). Observed boundary layer controls on shallow cumulus at the ARM Southern Great Plains site. *Journal of the Atmospheric Sciences*, 75(7), 2235–2255. <https://doi.org/10.1175/jas-d-17-0244.1>
- Lee, J. M., Zhang, Y., & Klein, S. A. (2019). The effect of land surface heterogeneity and background wind on shallow cumulus clouds and the transition to deeper convection. *Journal of the Atmospheric Sciences*, 76(2), 401–419. <https://doi.org/10.1175/jas-d-18-0196.1>
- Liu, Y., & Key, J. R. (2016). Assessment of Arctic cloud cover anomalies in atmospheric reanalysis products using satellite data. *Journal of Climate*, 29(17), 6065–6083. <https://doi.org/10.1175/jcli-d-15-0861.1>
- Miao, H., Wang, X., Liu, Y., & Wu, G. (2019). An evaluation of cloud vertical structure in three reanalyses against CloudSat/cloud-aerosol lidar and infrared pathfinder satellite observations. *Atmospheric Science Letters*, 20(7), e906. <https://doi.org/10.1002/asl.906>
- Moeng, C. H., Cotton, W. R., Bretherton, C., Chlond, A., Khairoutdinov, M., Krueger, S., et al. (1996). Simulation of a stratocumulus-topped planetary boundary layer: Intercomparison among different numerical codes. *Bulletin of the American Meteorological Society*, 77(2), 261–278. [https://doi.org/10.1175/1520-0477\(1996\)077<0261:soastp>2.0.co;2](https://doi.org/10.1175/1520-0477(1996)077<0261:soastp>2.0.co;2)
- Peng, X., She, J., Zhang, S., Tan, J., & Li, Y. (2019). Evaluation of multi-reanalysis solar radiation products using global surface observations. *Atmosphere*, 10(2), 42. <https://doi.org/10.3390/atmos10020042>
- Poll, S., Shrestha, P., & Simmer, C. (2022). Grid resolution dependency of land surface heterogeneity effects on boundary-layer structure. *Quarterly Journal of the Royal Meteorological Society*, 148(742), 141–158. <https://doi.org/10.1002/qj.4196>
- Qian, Y., Guo, Z., Larson, V. E., Leung, L. R., Lin, W., Ma, P. L., et al. (2023). Region and cloud regime dependence of parametric sensitivity in E3SM atmosphere model. *Climate Dynamics*, 62(2), 1–17. <https://doi.org/10.1007/s00382-023-06977-3>
- Randles, C. A., Da Silva, A. M., Buchard, V., Colarco, P. R., Darmenov, A., Govindaraju, R., et al. (2017). The MERRA-2 aerosol reanalysis, 1980 onward. Part I: System description and data assimilation evaluation. *Journal of climate*, 30(17), 6823–6850. <https://doi.org/10.1175/jcli-d-16-0609.1>
- Rieck, M., Hohenegger, C., & van Heerwaarden, C. C. (2014). The influence of land surface heterogeneities on cloud size development. *Monthly Weather Review*, 142(10), 3830–3846. <https://doi.org/10.1175/mwr-d-13-00354.1>
- Romps, D. M. (2017). Exact expression for the lifting condensation level. *Journal of the Atmospheric Sciences*, 74(12), 3891–3900. <https://doi.org/10.1175/jas-d-17-0102.1>
- Sakaguchi, K., Berg, L. K., Chen, J., Fast, J., Newsom, R., Tai, S. L., et al. (2022). Determining spatial scales of soil moisture—Cloud coupling pathways using semi-idealized simulations. *Journal of Geophysical Research: Atmospheres*, 127(2), e2021JD035282. <https://doi.org/10.1029/2021jd035282>
- Satoh, M., Tomita, H., Miura, H., Iga, S., & Nasuno, T. (2005). Development of a global cloud resolving model – A multi-scale structure of tropical convections. *Journal of the Earth Simulator*, 3, 11–19.
- Schneider, T., Kaul, C. M., & Pressel, K. G. (2019). Possible climate transitions from breakup of stratocumulus decks under greenhouse warming. *Nature Geoscience*, 12(3), 163–167. <https://doi.org/10.1038/s41561-019-0310-1>
- Schumacher, C., & Funk, A. (2023). Assessing convective-stratiform precipitation regimes in the tropics and extratropics with the GPM satellite radar. *Geophysical Research Letters*, 50(14), e2023GL102786. <https://doi.org/10.1029/2023gl102786>
- Su, H., Jiang, J. H., Zhai, C., Perun, V. S., Shen, J. T., Del Genio, A., et al. (2013). Diagnosis of regime-dependent cloud simulation errors in CMIP5 models using “A-Train” satellite observations and reanalysis data. *Journal of Geophysical Research: Atmospheres*, 118(7), 2762–2780. <https://doi.org/10.1029/2012jd018575>
- Su, T. (2023). Cloud regime identification over the SGP [Dataset]. *Zenodo*. <https://doi.org/10.5281/zenodo.10437096>
- Su, T., & Li, Z. (2023). Planetary boundary layer height (PBLH) over SGP from 1998 to 2023 [Dataset]. *ORNL; ARM Archive*. <https://doi.org/10.5439/2007149>
- Su, T., & Li, Z. (2024). Decoding the dialogue between clouds and land. *Eos*, 105. <https://doi.org/10.1029/2024EO240072>
- Su, T., Li, Z., & Kahn, R. (2020). A new method to retrieve the diurnal variability of planetary boundary layer height from lidar under different thermodynamic stability conditions. *Remote Sensing of Environment*, 237, 111519. <https://doi.org/10.1016/j.rse.2019.111519>
- Su, T., Li, Z., & Zheng, Y. (2023). Cloud-surface coupling alters the morning transition from stable to unstable boundary layer. *Geophysical Research Letters*, 50(5), e2022GL102256. <https://doi.org/10.1029/2022gl102256>
- Su, T., Zheng, Y., & Li, Z. (2022). Methodology to determine the coupling of continental clouds with surface and boundary layer height under cloudy conditions from lidar and meteorological data. *Atmospheric Chemistry and Physics*, 22(2), 1453–1466. <https://doi.org/10.5194/acp-22-1453-2022>
- Tang, S., Xie, S., Zhang, M., Tang, Q., Zhang, Y., Klein, S. A., et al. (2019). Differences in eddy-correlation and energy-balance surface turbulent heat flux measurements and their impacts on the large-scale forcing fields at the ARM SGP site. *Journal of Geophysical Research: Atmospheres*, 124(6), 3301–3318. <https://doi.org/10.1029/2018jd029689>
- Tao, C., Xie, S., Ma, H. Y., Bechtold, P., Cui, Z., Vaillancourt, P. A., et al. (2023). Diurnal cycle of precipitation over the tropics and central US: GCM intercomparison. *Quarterly Journal of the Royal Meteorological Society*, 150(759), 911–936. <https://doi.org/10.1002/qj.4629>
- Tao, C., Zhang, Y., Tang, Q., Ma, H. Y., Ghate, V. P., Tang, S., et al. (2021). Land–atmosphere coupling at the US Southern Great Plains: A comparison on local convective regimes between ARM observations, reanalysis, and climate model simulations. *Journal of Hydrometeorology*, 22(2), 463–481. <https://doi.org/10.1175/jhm-d-20-0078.1>
- Tao, C., Zhang, Y., Tang, S., Tang, Q., Ma, H. Y., Xie, S., & Zhang, M. (2019). Regional moisture budget and land-atmosphere coupling over the US Southern Great Plains inferred from the ARM long-term observations. *Journal of Geophysical Research: Atmospheres*, 124(17–18), 10091–10108. <https://doi.org/10.1029/2019jd030585>
- Teixeira, J., & Hogan, T. F. (2002). Boundary layer clouds in a global atmospheric model: Simple cloud cover parameterizations. *Journal of Climate*, 15(11), 1261–1276. [https://doi.org/10.1175/1520-0442\(2002\)015<1261:blciag>2.0.co;2](https://doi.org/10.1175/1520-0442(2002)015<1261:blciag>2.0.co;2)
- Tian, J., Zhang, Y., Klein, S. A., Öktem, R., & Wang, L. (2022). How does land cover and its heterogeneity length scales affect the formation of summertime shallow cumulus clouds in observations from the US Southern Great Plains? *Geophysical Research Letters*, 49(7), e2021GL097070. <https://doi.org/10.1029/2021gl097070>
- Tiedtke, M. (1993). Representation of clouds in large-scale models. *Monthly Weather Review*, 121(11), 3040–3061. [https://doi.org/10.1175/1520-0493\(1993\)121<3040:rocils>2.0.co;2](https://doi.org/10.1175/1520-0493(1993)121<3040:rocils>2.0.co;2)
- Wang, Y., Hu, J., Li, R., Song, B., Hailemariam, M., Fu, Y., & Duan, J. (2023). Increasing cloud coverage deteriorates evapotranspiration estimating accuracy from satellite, reanalysis and land surface models over East Asia. *Geophysical Research Letters*, 50(8), e2022GL102706. <https://doi.org/10.1029/2022gl102706>

- Xian, T., Guo, J., Zhao, R., Su, T., & Li, Z. (2023). The impact of urbanization on mesoscale convective systems in the Yangtze River Delta region of China: Insights gained from observations and modeling. *Journal of Geophysical Research: Atmospheres*, *128*(3), e2022JD037709. <https://doi.org/10.1029/2022jd037709>
- Xiao, H., Berg, L. K., & Huang, M. (2018). The impact of surface heterogeneities and land-atmosphere interactions on shallow clouds over ARM SGP site. *Journal of Advances in Modeling Earth Systems*, *10*(6), 1220–1244. <https://doi.org/10.1029/2018ms001286>
- Xie, S., McCoy, R. B., Klein, S. A., Cederwall, R. T., Wiscombe, W. J., Clothiaux, E. E., et al. (2010). Clouds and more: ARM climate modeling best estimate data: A new data product for climate studies. *Bulletin of the American Meteorological Society*, *91*(1), 13–20. <https://doi.org/10.1175/2009bams2891.1>
- Yang, Y. J., Wang, H., Chen, F., Zheng, X., Fu, Y., & Zhou, S. (2019). TRMM-based optical and microphysical features of precipitating clouds in summer over the Yangtze–Huaihe River valley, China. *Pure and Applied Geophysics*, *176*(1), 357–370. <https://doi.org/10.1007/s00024-018-1940-8>
- Yue, Q., Kahn, B. H., Fetzner, E. J., Wong, S., Frey, R., & Meyer, K. G. (2017). On the response of MODIS cloud coverage to global mean surface air temperature. *Journal of Geophysical Research: Atmospheres*, *122*(2), 966–979. <https://doi.org/10.1002/2016jd025174>
- Zhang, Y., & Klein, S. A. (2010). Mechanisms affecting the transition from shallow to deep convection over land: Inferences from observations of the diurnal cycle collected at the ARM Southern Great Plains site. *Journal of the Atmospheric Sciences*, *67*(9), 2943–2959. <https://doi.org/10.1175/2010jas3366.1>
- Zhang, Y., & Klein, S. A. (2013). Factors controlling the vertical extent of fair-weather shallow cumulus clouds over land: Investigation of diurnal-cycle observations collected at the ARM Southern Great Plains site. *Journal of the Atmospheric Sciences*, *70*(4), 1297–1315. <https://doi.org/10.1175/jas-d-12-0131.1>
- Zhang, Y., Klein, S. A., Fan, J., Chandra, A. S., Kollias, P., Xie, S., & Tang, S. (2017). Large-eddy simulation of shallow cumulus over land: A composite case based on ARM long-term observations at its Southern Great Plains site. *Journal of the Atmospheric Sciences*, *74*(10), 3229–3251. <https://doi.org/10.1175/jas-d-16-0317.1>
- Zheng, Y., Zhang, H., Rosenfeld, D., Lee, S. S., Su, T., & Li, Z. (2021). Idealized large-eddy simulations of stratocumulus advecting over cold water. Part I: Boundary layer decoupling. *Journal of the Atmospheric Sciences*, *78*(12), 4089–4102.

## References From the Supporting Information

- Holdridge, D., Ritsche, M., Prell, J., & Coulter, R. (2011). Balloon-borne sounding system (SONDE) handbook. Retrieved from <https://www.arm.gov/capabilities/instruments/sonde>
- Liu, S., & Liang, X. Z. (2010). Observed diurnal cycle climatology of planetary boundary layer height. *Journal of Climate*, *23*(21), 5790–5809. <https://doi.org/10.1175/2010jcli3552.1>
- Schaaf, C. B., Gao, F., Strahler, A. H., Lucht, W., Li, X., Tsang, T., et al. (2002). First operational BRDF, albedo nadir reflectance products from MODIS. *Remote Sensing of Environment*, *83*(1–2), 135–148. [https://doi.org/10.1016/s0034-4257\(02\)00091-3](https://doi.org/10.1016/s0034-4257(02)00091-3)
- Wesely, M. L., Cook, D. R., & Coulter, R. L. (1995). *Surface heat flux data from energy balance Bowen ratio systems* (No. ANL/ER/CP-84065; CONF-9503104-2). Argonne National Laboratory.